Iraqi Journal of Science, 2019, Vol. 60, No. 4, pp: 677-687
DOI: 10.24996/ijs.2019.60.4.1

ISSN: 0067-2904

Thermodynamics and Kinetics of Hydrogen Transfer Mechanism in1-[(E)-1, 3-Benzothiazol-2-Ylazo]Naphthalen-2-Ol Tautomers in Aqueous Medium/ Density Functional Theory

Ibrahim Asiata Omotayo[1], Oyebamiji Abel Kolawole[1,2], Semire Banjo[1]*
[1]Department of Pure and Applied Chemistry, Ladoke Akintola University of Technology, P.M.B. 4000, Ogbomoso, Oyo state, Nigeria.
[2]Department of Basic Science, Faculty of Sciences, Adeleke University, P.M.B. 250, Ede, Osun State, Nigeria

Abstract

Enol-Keto tautomerism in 1-[(E)-1,3-benzothiazol-2-ylazo]naphthalen-2-ol has been studied using the B3LYP functional of density functional theory (DFT) with 6-31G(d,p) basis set. Relative and absolute energies, transition state geometries (TS), dipole moments, entropies, enthalpies and Gibbs free energies, equilibrium constants (K_T) and rate of tautomerization (k_r) were calculated. Also, the computations of geometries and vibration frequencies for the tautomers were calculated and compared. The results of the calculations showed that the enol form is the most stable form than other isomers, this might be due to intra-hydrogen bonding. The TS1 activation energies for tautomer A ↔ B, tautomer A ↔ C and tautomer B ↔ C are 92.65, 199.56 and 225.71 kJ/mol respectively. The TS1 is lower than TS2 by 102 kJ/mol, showing that A ↔ B and B ↔ C paths are thermodynamic control and A ↔ C path is a kinetic control. The overall calculated $K_T \approx 1$, indicating that all tautomers present in significant proportions.

Keywords: Azo dyes, Tautomerization, Activation energy, DFT.

1. Introduction

Among other dyes, azo-dyes are of particular interest for chemists because they can be easily prepared with a wide range of donor and acceptor substituent. In addition, the planarity of the azo bridge is expected to contribute to enhancing electronic delocalization, and consequently, the optical activity [1]. Azo-dyes can be used in several analytical and biochemical applications such as redox, metallochromic acid-base indicators [2] and protein binder [3]. The interest of studying the tautomerism of heterocyclic compounds has grown in the past two decades due to the influence of tautomerism on chemical and biological activities. Enol- and keto-tautomers of azo dyes was first observed in 1884 by Zince and Bindenwald [4]. It although equilibrium ($K_e = \frac{[keto]}{[enol]}$) tautomeric ratio is a solvent and a temperature dependent, theses tautomers may co-exist in a solution due to fast proton exchange [5-7]. The tautomeric form of azo dyes has been found to play a crucial role in designing efficient oxidation processes; which could minimize the toxicological effects such as the formation of carcinogenic amines [8].

The recent investigations of tautomeric azo-naphthols are due to their differences in properties which should be made possible to be isolated. However, it has been shown that they are impossible to isolate individual tautomers by equilibrium switching [9,10]. Adequate knowledge about the molecular structure of a dye is key to understand its chemical and physical properties. Quantum-chemical calculations are a veritable tool to study the tautomeric compounds, yet, the accuracy of the results might highly depend on the theories that have been used [11,12].

*Email: bsemire@lautech.edu.ng

In one of our recent papers, we reported the electronic properties and the reactivity of 4-[(Z)-[4-(triflоromethyl)-1,3-benzothiazol-2-yl]azo]naphthalen-1-ol (*ortho*-OH) and 1-[(Z)-[4-(triflоromethyl)-1,3-benzothiazol-2-yl]azo]naphthalen-2-ol (*para*-OH)using Density Functional Theory (B3LYP/6-31G*). The results revealed that structural relaxation was observed in para-OH isomer which led to thermodynamic stability for *ortho*-OH by 26.34kJ/ molover *para-OH* [13]; this was not in agreement with the reported experimental in the literature [14]. The stability of *ortho*-OH over *para*-OH could be attributed to hydrogen bond in the plane between one azo-nitrogen and *para* hydroxyl hydrogen (N---HO; 1.962 Å) which would lead to tautomerization in *ortho-OH*. Therefore, analysis of geometrical and energetic changes of 3-[(E)-1,3-benzothiazol-2-ylazo]naphthalen-2-oltautomers that caused by the migration of hydrogen atom are necessary to gain an insight into the electronic properties of the tautomers.

In the present work, a quantum chemical method of Density Functional Theory(DFT) was used to study the mechanism of hydrogen transfer in tautomers, the geometrical structures, the electronic properties, and to calculate the tautomerization constant of the tautomers:1-[(E)-1,3-benzothiazol-2-ylazo]naphthalen-2-ol (A), (1E)-1-(1,3-benzothiazol-2-ylhydrazono)naphthalen-2-one (B) and (1E)-3-[(E)-3H-1,3-benzothiazol-2-ylidenehydrazono]naphthalen-2-one(C). Therefore, the tautomeric change in thermodynamics, equilibrium and kinetics properties are estimated from the theoretical point of view using (DFT) in aqueous medium. The schematic illustration of inter-conversion of 1-[(E)-1, 3-benzothiazol-2-ylazo]naphthalen-2-ol tautomers through transition state are shown in scheme 1.

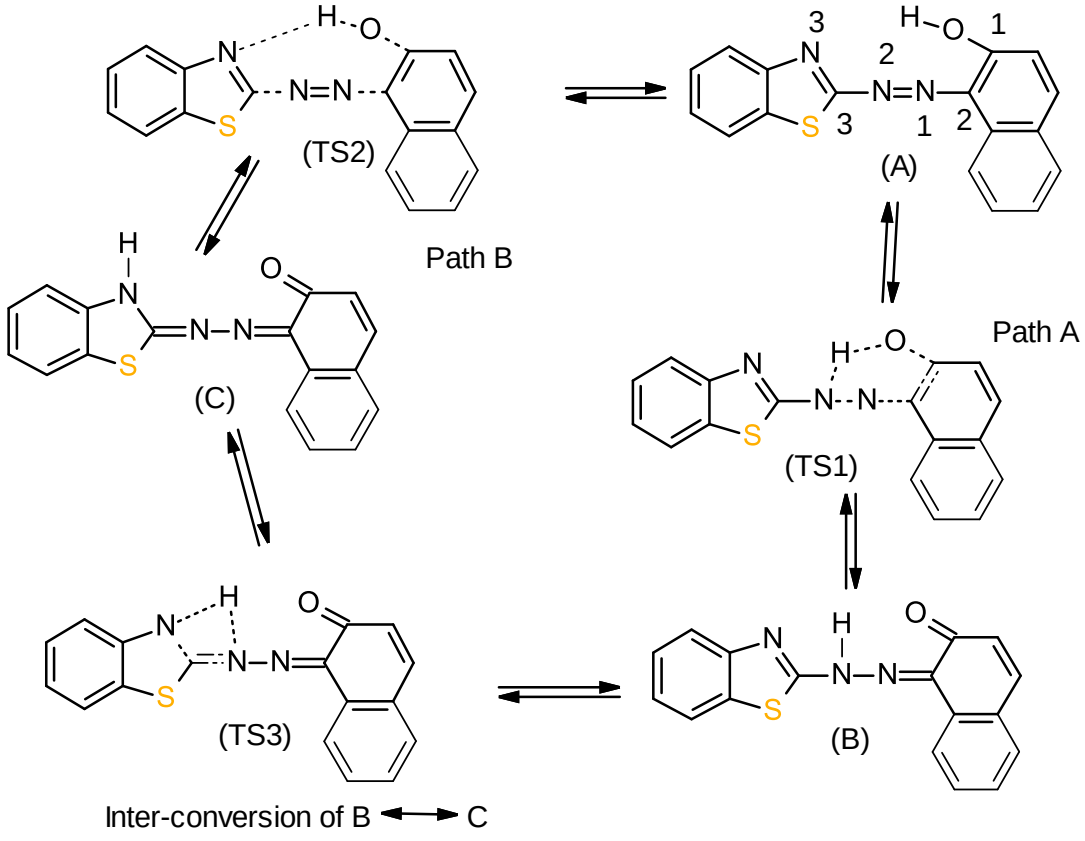

Scheme 1-Tautomerization through transition states TS1, TS2 and TS3 with atoms numbering.

2. Computational methods

The conformation search on 1-[(E)-1,3-benzothiazol-2-ylazo]naphthalen-2-ol and its tautomers were performed using semiempirical AM1 method Monte Carlo search algorithm and the lowest energy conformer of its conformational search was taken for DFT calculations [15]. The equilibrium geometry calculations were performed at density functional theory (Beckes's three-parameter hybrid functional [16] employing the Lee, Yang and Parr correlation functional B3LYP [17]). Molecular properties and vibrational frequencies calculations for these molecules were performed at the same level of theory, however, the optimized structures in the gas phase were used for energy calculations in

aqueous medium. The convergence criteria for the geometry optimization and energy calculations are as in default parameters of the Spartan 14 program.

The reactivity of tautomers that are predicted based on DFT concept, ionization potential (IP) and electron affinity (EA) are determined using the energy variation for the compound derived from the electron transfer which could be approximated as; IP ≈ -E_{HOMO} and EA ≈ -$E_{LUMO,}$ respectively, based on Koopman's theorem [18]. The chemical hardness (η), the chemical potential (μ), softness (1/η) and electrophilicity index (ω) of a molecule are deduced form IP and EA values [19-25], this is shown in equations 1, 2 and 3:

$$\mu = -\chi = \left(\frac{\partial E}{\partial N}\right) v(r) \approx \frac{1}{2}[IP + EA] \approx \frac{1}{2}[E_{HOMO} + E_{LUMO}] \quad (1)$$

$$\eta = \left(\frac{\partial^2 E}{\partial N^2}\right) v(r) \approx \frac{1}{2}[IP - EA] \approx \frac{1}{2}[E_{HOMO} - E_{LUMO}] \quad (2)$$

$$\omega = \frac{\mu^2}{2\eta} \quad \textbf{(3)}$$

Thermodynamic parameters, equilibrium compositions and kinetics properties of tautomerization were calculated according to the following equations:

$$\Delta \boldsymbol{G}^{\circ}_{\boldsymbol{rxn}} = \boldsymbol{\Delta H}^{\circ}_{\boldsymbol{rxn}} - \boldsymbol{T\Delta S}^{\circ}_{\boldsymbol{rxn}} \quad \textbf{(4)}$$

Where $\Delta G^{\circ}_{rxn}, \Delta H^{\circ}_{rxn} and \Delta S^{\circ}_{rxn}$ arethechange in free energy,enthalpy and entropy between the most stable tautomer and that of the less stable onece.

$$\Delta G^{\circ}_{rxn} = -RTlnK_T \quad \textbf{(5)}$$

K_T is the equilibrium constant, R is the gas constant, T =298 K

$$K_T = e^{\left(\frac{\Delta G^{\circ}_{rxn}}{RT}\right)} \quad \textbf{(6)}$$

The rate constant (k_{rxn}) for the tautomerization is obtained directly from the activation energy, ΔE*, according to equation 7:

$$k_{rxn} = \frac{K_b T}{h} e^{\left(\frac{-\Delta G^*}{RT}\right)} \quad \textbf{(7)}$$

K_b is the Boltzmann constant, h is the Planck's constant, and $\Delta G^{\#}$is the difference in energy of the transition state and stable tautomer,

At room temperature and when ΔG* is in kJ/mol, K_{rxn} is given by:

$$k_{rxn} = 6.20x10^{12} * e^{\left(\frac{-\Delta G^*}{RT}\right)} \quad \textbf{(8)}$$

Also, the ratio of the tautomers is used to be calculated to establish the equilibrium composition of a mixture of tautomers such that:

$$\%\, Tautomer\ (i) = \frac{100 e^{-1060 E_{Tautomer\ (i)}}}{\sum_k e^{-1060 E_{Tautomer\ (k)}}} \cong \frac{100\, K_{Tautomer(i)}}{\sum_k K_{Tautomer(k)}} \quad \textbf{(9)}$$

Tautomer energies ($E_{tautomer}$), given in atomic units, represent the energy of the lowest-energy isomer.

3. Results and discussion

3.1 Optimized geometries

The optimized 3-[(E)-1,3-benzothiazol-2-ylazo]naphthalen-2-ol tautomers and their inter-conversion transition states at B3LYP/6-31G* levels of theory are displayed in Figure-1. Geometries parameters (bond lengths, bond angles, and dihedral angles) that are calculated for these compounds are listed in Table-1. The C1-C2 bond distance is 1.421Å for A, 1.523Å for B and 1.522Å for C, respectively. The observed increase in C1-C2 bond distance for B and C compared to A is due to the decrease in double bond character. Similarly, the decrease in N1-C2 bond distance is due to the increase in bond force constant as a result of the increase in double bond nature in molecules B and C, Table-1. Comparing the compound of 1-[(E)-1,3-benzothiazol-2-ylazo]naphthalen-2-ol (A), and compound (1E)-1-(1,3-benzothiazol-2-ylhydrazono)naphthalen-2-one (B) in this work to 1-[(E)-1,3-benzothiazol-6-ylazo]naphthalen-2-ol and (1E)-1-(1,3-benzothiazol-6-ylhydrazono)naphthalen-2-one [8],the calculated C2-N1, N2-C3 and C3-N3 bond distances are 1.372, 1.394 and 1.295 Å for compound (A),and 1.303, 1.384 and 1.292 Å for compound (B), respectively. These bonds were calculated to be 1.382, 1.411 and 1.289 Åfor 1-[(E)-1,3-benzothiazol-6-ylazo]naphthalen-2-ol,and 1.325, 1.401 and 1.288 Å for (1E)-1-(1,3-benzothiazol-6-ylhydrazono)naphthalen-2-one [8].Also, the

bond angles (C2-N1, C2-N3, and C3-N3) are 1.346, 1.382 and 1.294Å for TS1; 1.327, 1.239 and 1.371Å for TS2; 1.315, 1.345 and 1.330Å for TS3, respectively.

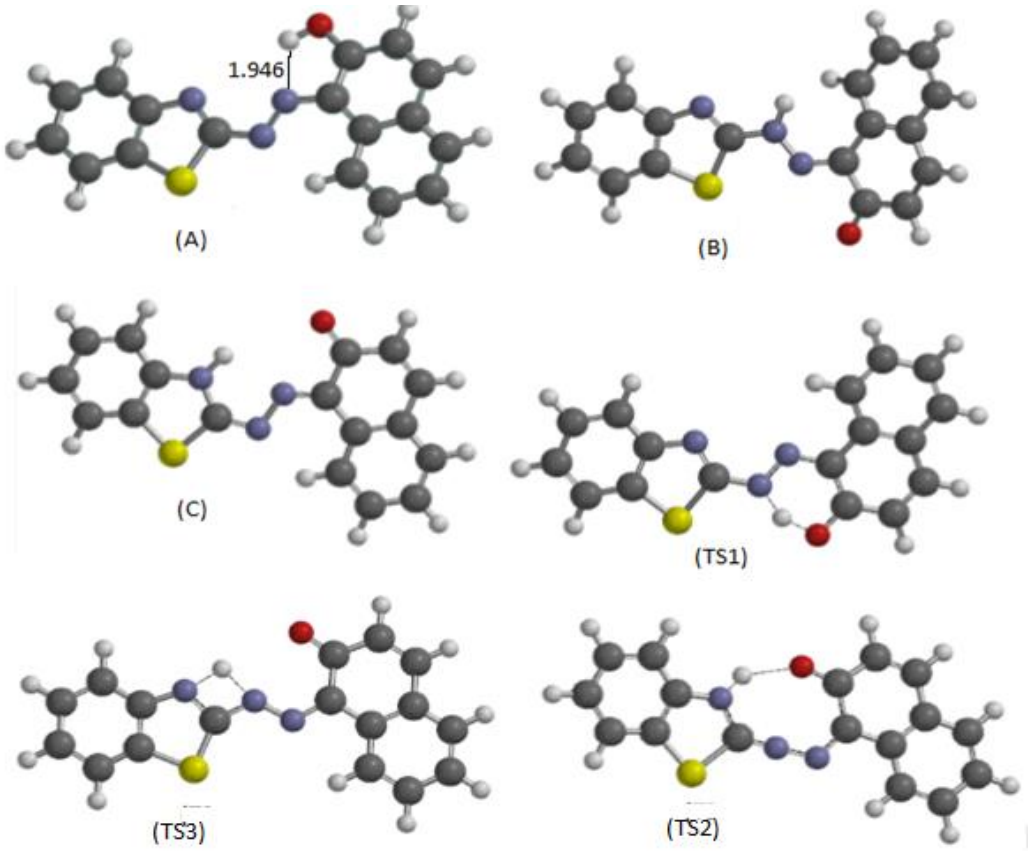

Figure 1-Optimized structures of the studied tautomers and their inter-conversion transition states.

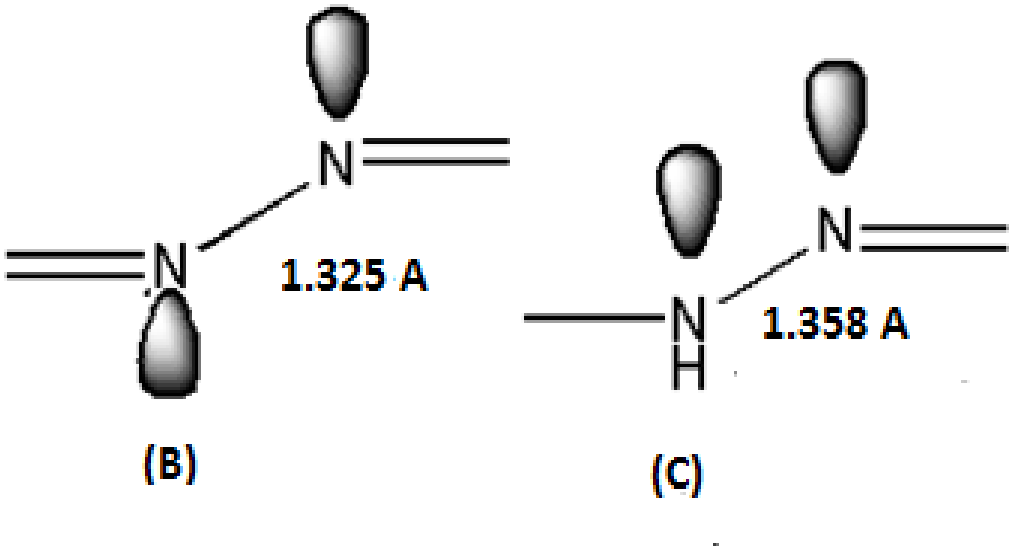

Scheme 2-he possible positions of the lone pair electrons on molecules (B) and (C)

The N-N bond distance for (A), (B) and (C) are 1.274, 1.325 and 1.358Å, respectively, These are bigger if compared to 1.272Å for 1-[(E)-1,3-benzothiazol-6-ylazo]naphthalen-2-ol and 1.306Å for (1E)-1-(1,3-benzothiazol-6-ylhydrazono)naphthalen-2-one [8]. However, the average Ar-N=N-Ar bond distance has been reported to be 1.255Å [26], thus, Ar-N=N-Ar in compound A is lengthened by 0.019 Å which is comparable to 1.271 previously reported for 1-trifluoromethyl-4-

dimethylaminoazobenzene [27]. The difference in N-N bond distance for (B) and (C) (in spite that N-N is a single bond in both B and C) is due to the positions/arrangement of lone pair electrons on the nitrogen atoms (see scheme 2). N-N bond distance is 1.304, 1.305 and 1.316Å for TS1, TS2 and TS3, respectively. The arrangement of lone pair electrons on the N-N atoms in (C) is also accounted for the lengthening of N-N bond distance in TS2 compared to TS1 and TS3 (scheme 2). The bond angle of 1-[(E)-1,3-benzothiazol-2-ylazo]naphthalen-2-ol and its tautomers as well as the transition states are different due to differences in geometrical structures of the molecules. For instance, C1C2N1 and N1N2C3 bond angles are 109.73 and 112.77° for (A), 117.13 and 119.34° for (B) and 110.68 and 108.68° for (C). These bond angles are 121.98 and 117.80 for TS1, 124.27 and 122.47 for TS2 and 126.45 and 178.64 for TS3, the bond angle in the transition states increased than the tautomers. The calculated dihedral angles show that the tautomers and the transition state geometries are planar; except molecule (B) which slightly distorts from planarity, Table-1.

Table 1-Selected geometrical parameters for tautomers and the transition states

Geometry	A	TS1	B	TS2	C	TS3
C1-O	1.334	1.285	1.227	1.243	1.231	1.236
C1-C2	1.421	1.444	1.523	1.498	1.522	1.496
C2-N1	1.372	1.346	1.303	1.327	1.303	1.315
N1-N2	1.274	1.304	1.325	1.305	1.358	1.316
N2-C3	1.394	1.382	1.384	1.239	1.315	1.345
C3-N3	1.295	1.294	1.292	1.371	1.358	1.330
C3-S	1.770	1.775	1.776	1.874	1.761	1.736
O-N1	2.553	-	2.688	-	2.610	-
O-H1		1.904		1.829		-
N2-H1		1.266	1.029	-		1.431
N3-H1		-		1.029	1.009	1.338
OC1C2	120.35	120.06	122.69	124.04	122.06	122.85
C1C2N1	109.73	121.98	112.13	126.45	110.68	124.27
C2N1N2	121.26	115.65	122.81	120.72	121.81	120.80
N1N2C3	112.77	117.80	119.34	178.69	108.68	122.47
N2C3N3	129.30	127.42	121.62	127.64	126.10	104.42
N2C3S	114.44	116.00	120.00	126.39	122.36	140.04
OC1C2N1	0.06	0.00	16.24	0.00	0.00	-0.70
C1C2N1N2	179.94	0.00	175.70	0.00	180.00	-0.14
C2N1N2C3	-179.81	180.00	-176.00	0.00	180.00	179.93
N1N2C3N3	0.30	0.00	175.97		0.00	0.00
N1N2C3S	-179.77	180.00	-5.33		180.00	180.00

3.2 Vibration frequencies

Vibrational spectroscopy is being used fororganic compoundscharacterization;this includes identification of functional groups and distinguishing molecular conformers and tautiomers. In quell to understand fairly complex systems, experimental vibrational modes coupled with theoretical results are now commonly used. Therefore in this work, theoretically calculated vibrational frequencies of tautomers (A), (B) and (C) are compared with other results for similar isomers calculated at the same level of the theory. The theoretical vibrational frequency values and the spectra of B3LYP/6-31G(d,p) level for three tautomers of (A), (B) and (C) are displayed in Table-2 and Figure-2, respectively. For

effective comparison, these compounds are compared with similar isomeric tautomers of1-[(E)-1,3-benzothiazol-6-ylazo]naphthalen-2-ol (D) and (1E)-1-(1,3-benzothiazol-6-ylhydrazono)naphthalen-2-one (E) which were reported by Pavlovic et al., [8]. The N-H and O-H vibrational frequency values showed a similar band profile. The calculated N-H was 3455cm^{-1}with 15.42 intensity for tautomer (B), 3478 cm^{-1}with 56.04 intensity for tautomer C compared to 3445cm^{-1}with 5.93km/mol intensity forE.*ν*O-H for A and D are 3415 and 3505cm^{-1}with intensities of 54.98km/mol and 147.06km/mol, respectively. Also, 3443 cm^{-1} was observed for similar compound of 4-[(E)-[4-(trifloromethyl)-1,3-benzothiazol-2-yl]azo]naphthalen-1-ol [13].σN-Hbandscalculated at 629 and 691 cm^{-1} are assigned for tautomers (B) and (C), respectively, whereas for (E), it was calculated to be 643 and 562 cm^{-1}. The calculated O-H and N-H vibrational frequencies for D and (E) are 3445cm^{-1}and 3505cm^{-1} respectively. The *ν*N-H experimentally observed at 3433cm^{-1}for E. The calculated N=N stretching vibrations were 1484cm^{-1} for (A) and 1513, 1469 and 1443cm^{-1} for (D), however, N-N stretching vibrations were calculated to be 1186cm^{-1} for (B), 1247, 1148 and 1091cm^{-1} for B, and 1310 and 1185 cm^{-1} for (E). The O–H out-of-plane, bending vibrations were calculated to be 818 and 931cm^{-1} for (A) and (D), respectively.

The aromatic C–H stretching vibrations for tautomers (A), (B) and (C) were calculated to be in the regions of 3232-3085, 3209-3054 and 3278-3048cm^{-1} respectively. They were also calculated for (D) and E in the regions of 3240-3179 and 3238-3170cm^{-1}, respectively, and was experimentally observed for (E) at 3039 cm^{-1} [8] and 3055-3051 cm^{-1} for 4-[(E)-[4-(trifloromethyl)-1, 3-benzothiazol-2-yl]azo]naphthalen-1-ol [13]. C–S stretching vibrations were calculated to be: 1231, 1068 and 716 cm^{-1} for A,1333, 1076, 713 and 699 cm^{-1} for B, and 1320, 1074 and 707 cm^{-1} for C. These were calculated at 1056, 814, 669 and 647 cm^{-1} for D, and 1057 and 662 cm^{-1} for E.νC=O stretching vibrations were calculated at 1757, 1733 and 1748 cm^{-1} for B, C and E, respectively. The aromatic bond of C=C which is coupled with C=N stretching vibrations for the tautomers A, B and C were calculated to be in the regions of 1642 and 1543 cm^{-1} for A; 1607 and 1598 cm^{-1} for B, and 1626 and 1537 cm^{-1} for C. They were calculated at 1657, 1647, 1619, 1609 and 1546 cm^{-1} for D, however, it was previously reported at 1621 cm^{-1}[8]. For E, it was calculated at 1639, 1592, 1571 and 1540 cm^{-1}. They were also observed at 1624, 1610 and 1512 cm^{-1} for 4-[(E)-[4-(trifloromethyl)-1,3-benzothiazol-2-yl]azo]naphthalen-1-ol [13]. Within the limitation of the theoretical method used, the calculated vibrational frequencies agreed with the experimental data. However, the calculated frequencies are observed to be slightly higher than the experimental data due to environmental conditions, and the fact that experimental is an inharmonic frequency whereas the theoretical is a harmonic frequency. Theoretical results can be improved as compared to experimental data by scaling the theoretical results [28-32].

Table 2- Selected vibrational frequencies of the studied tautomers at DFT/B3LYP/6-31G(d,p)

A	B	C	Assignemnt
-	3455 (15.42km/mol)	3478 (56.04km/mol)	ν(N-H)
3415 (54.98)	-	-	νOH
3232-3085	3209-3054	3278-3048	νC-H
-	1757 (201.58km/mol)	1733 (194.51km/mol)	νC=O
1642, 1543	1607, 1598	1626, 1537	νC=C + νC=N
-	1461	1411	πN-H + νC=N
1231	1333	1320	νC-S
1275	-	-	πOH + πC-H
-	1265	1272	νC-NH
1484	-	-	νN=N
-	1186	1247, 1148, 1091	νN-N
1068, 1077	1076	1074	νC-S
818	-	-	σOH

716	699, 713	707	νC-S
-	629	691	σN-H

ν, stretching; π, in-plane bending; σ, out plane bending; *frequencies in bracket are taken from reference[8].

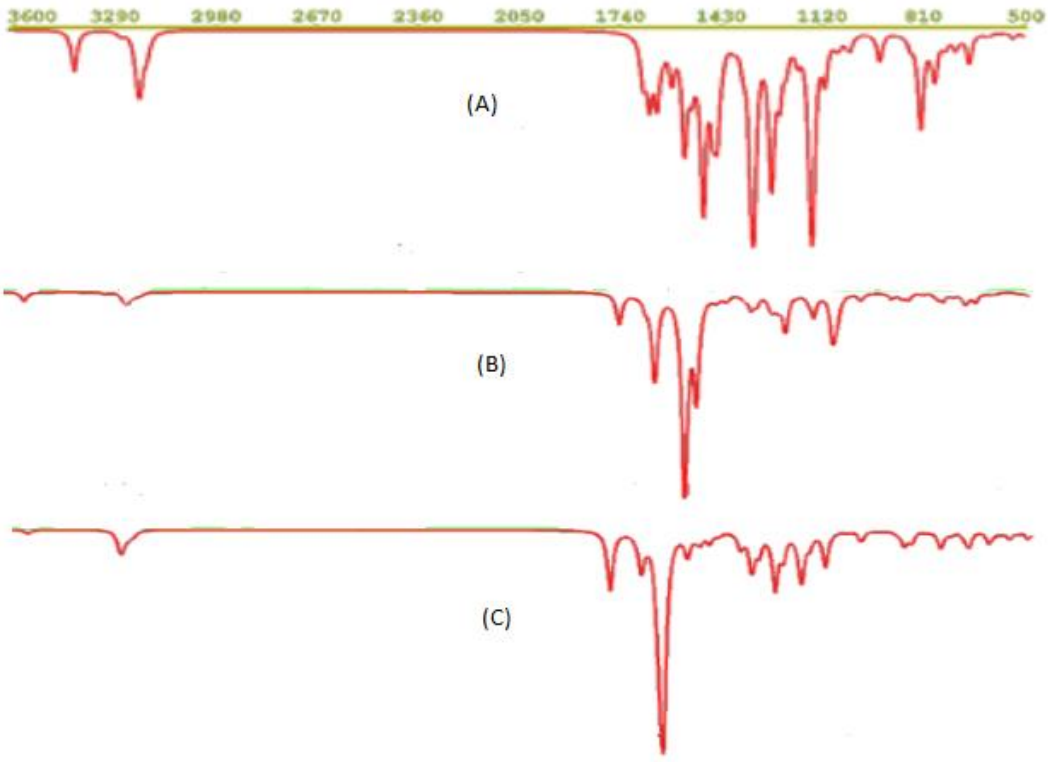

Figure 2-Simulated IR spectra at DFT/B3LYP/6-31G(d,p).

3.3 Stability and Equilibrium properties

The total and relative energies at DFT/6-31G (d,p) level of the tautomers of 1-[(E)-1,3-benzothiazol-2-ylazo]naphthalen-2-ol are presented in Table-3. Since it is the most stable tautomer (A) is taken as a reference to obtain the relative energetic stability of the other two tautomers. The total energies of (A), (B) and (C) are -1292.10124, -1292.0836 and -1292.09105au, respectively, indicating that (A) is relatively more stable tautomer than B and C by 46.24 and 26.75 kJ/mol, respectively. Thus, the order of stability are (A) > (C) > (B). This means that enol tautomer is stable and this may be due to hydrogen bond formation between –OH and N1 (-OH - - - N1; 1.946 Å).

The HOMO, LUMO and frontier molecular orbital energy gap ($\Delta E_{HOMO-LUMO}$), shown in Figure-3, for the tautomers are: -5.71, -280 and 2.91eV for A; -5.79, -2.67 and 3.12eV for (B); -5.54, -2.44 and 31.0eV, respectively. ΔE_g, η, and σ show that the tautomer has lowest band gap energy, chemical hardness and highest softness, thus, (A) is expected to be more reactive and more electrophilic (ω = 3.118 eV) than other tautomers. This is in agreement with the low value of LUMO energy and the order of stability; indicating tautomer A can readily accept an electron from the aqueous medium. This means (A) > (B) > (C). The magnitude of the dipole moment is inversely related to the tautomeric stability. The calculated dipole moments of the studied tautomers are found to be 1.43, 2.79 and 4.63Debye for enol tautomer (A), keto (C) and keto (B), respectively. The highest value of the dipole moment was found in case of keto (B) while the lowest one was found in the case of enol (A) [33]. The dipole moments for TS1, TS2, and TS3 are 1.32, 1.78 and 4.79Debye, respectively. This corresponds to the change in ΔE_g between the stable tautomers (ΔE_g) and the transition states. $\Delta Eg_{(A \leftrightarrow TS1)}$, $\Delta E_{g(A \leftrightarrow TS2)}$ and $\Delta E_{g(B \leftrightarrow TS3)}$ are 0.67, 0.78 and 1.11 eV, respectively, this means that the barrier high for A ↔ B is expected to be lower than the barrier high for A ↔ C, likewise, the barrier high for A ↔ C is also expected to be lower than that for B ↔ C.

Transition state (TS) for the reaction mechanism is explored by locating the stationary point on the potential energy surface at B3LYP/6-31G(d.p) level. The activation energy barrier for the tautomerization of A ↔ B through TS1 is 92.65 kJ/mol and for A ↔ C through TS2 is 199.56.Theinter-conversion of B ↔ C through TS3 is 225.71 kJ/mol (see Figure-4). These values agree with the change in ΔEg between the stable tautomers (ΔE_g) and the transition states (TS). TS1 for A ↔ B is lower than that of A ↔ C by 102 kJ/mol, indicating that A ↔ B path is a thermodynamic control, whereas A ↔ C path is a kinetic control. TS3 for B ↔ C is about 25 kJ/mol, this is higher than A ↔ C process, therefore, the inter-conversion of B ↔ Cwill be grossly solvent assisted which may lead to spontaneous process. The mole fraction of the tautomers (azo, A and hydrazine, B and C) in aqueous are: 0.3364 (33.64 %) for A, 0.3306 (33.06 %) for B and 0. 3330 (33.30 %) for C. The rates of inter-conversion show a magnitude of 10^{12}, this agrees with the estimated mole fraction of the tautomers. Though, the ratio of the two tautomers is described by the equilibrium constant $K_{T,}$ and its computed absolute values. $K_T > 1$ indicating a preference for the enol tautomer (A) relative to the keto ones (B) and (C). However, the absolute value of K_T highly depends on the accuracy of the evaluation of the free energy, also, determinate the privileged direction of equilibrium.

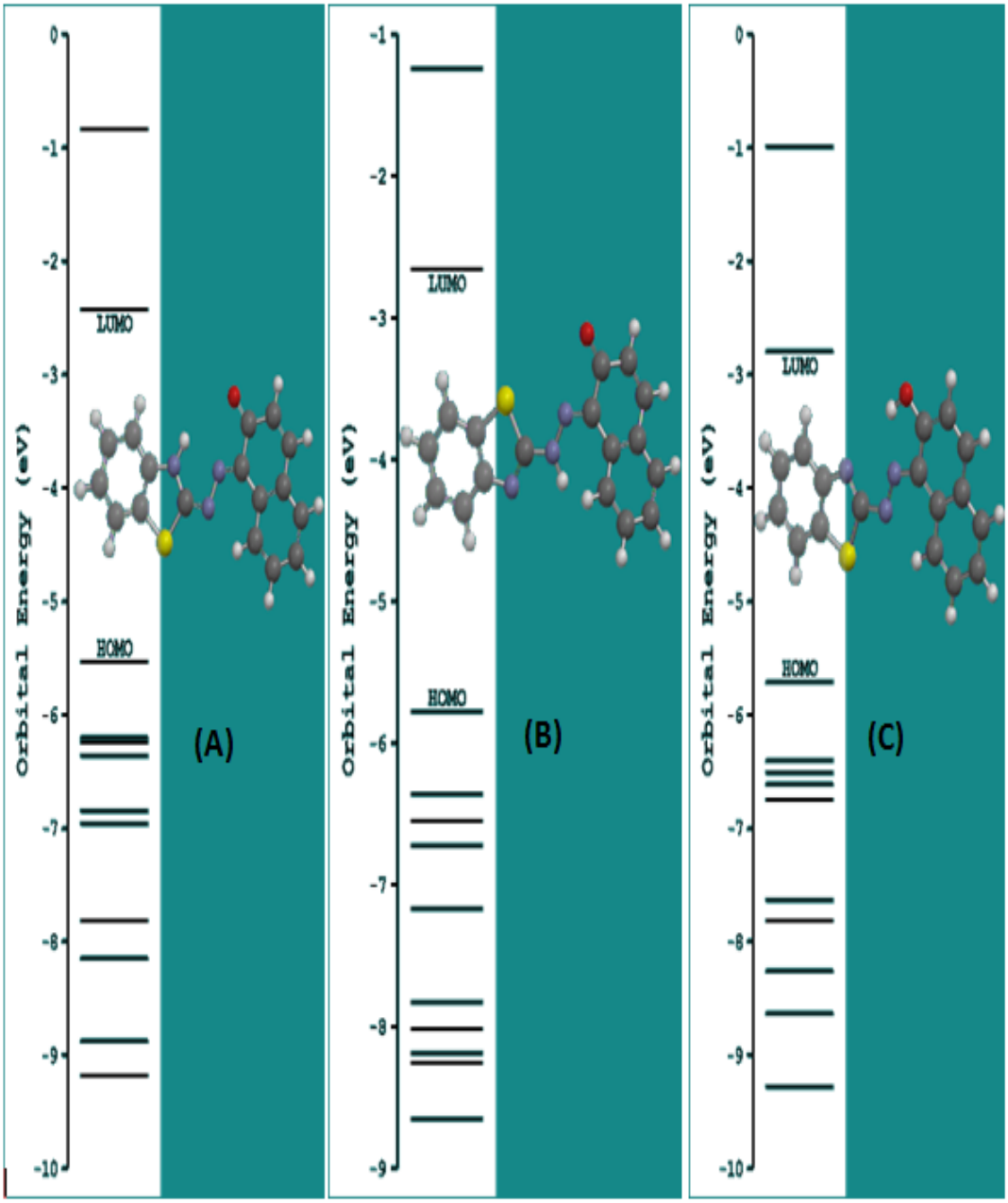

Figure 3-HOMO, LUMO and Frontier Molecular orbital energies diagrams.

Table 3-Electronic properties of the tautomers and the transition state complexes in aqueous solution

	A	B	C	TS1	TS2	TS3
Total energy (au)	-1292.10124	-1292.0836	-1292.09105	-1292.06595	-1292.02528	-1292.00508
Energy diff. (au)/kJ/mol	0.00/0.00	0.01761/ 46.24	0.01019/ 26.75	0.03529/ 92.65	0.07601/ 199.56	0.09616/ 225.71
$E_{HOMO\ (eV)}$	-5.71	-5.79	-5.54	-5.45	-5.07	-4.87
$E_{LUMO\ (eV)}$	-2.80	-2.67	-2.44	-3.21	-2.94	-2.88
$\Delta E_g = E_{HOMO} - E_{LUMO}$(eV)	2.91	3.12	3.10	2.24	2.13	1.99
η (eV)	1.455	1.560	1.550	1.120	1.065	0.995
μ (eV)	-4.26	-4.22	-3.99	-4.33	-4.005	-3.875
Softness = (1/η)	0.687	0.641	0.645	0.893	0.939	1.009
ω (eV)	3.118	2.854	2.560	4.185	3.765	3.773
D.M (Debye)	1.43	4.63	2.79	1.32	1.78	4.79
ZPE° (kJ/mol)	643.31	643.23	642.96	630.87	636.01	626.32
H°(kJ/mol)	682.91	683.34	682.92	675.33	680.87	672.24
S°(J/mol)	489.99	493.12	492.27	544.17	548.81	556.17
G°(kJ/mol)	536.82	536.31	536.15	513.09	517.24	506.42
fraction of Tautomer	0.3364	0.3306	0.3330			
% Composition	33.64	33.06	33.30			

Table 4- Equilibrium and kinetics parameters in aqueous solution

	ΔG°_{rxn}au (kJ/mol)	ΔE* au (kJ/mol)	ΔG^{*}(au)	K_T	k_r (10^{12})
A ⟷ B	-1.94×10^{-4} (-0.51)	-0.03529 (-92.65)	-9.04×10^{-3} (-2.374)	1.002059	6.14
A ⟷ C	-2.55×10^{-4} (-0.67)	-0.07601 (-199.56)8	-9.46×10^{-3} (-2.484)	1.000271	6.14
B ⟷ C	-5.09×10^{-5} (-0.134)	-0.08597 (-225.71)	-1.14×10^{-2} (-2.993)	1.000054	6.13

1 au = 2625.5kJ/mol.

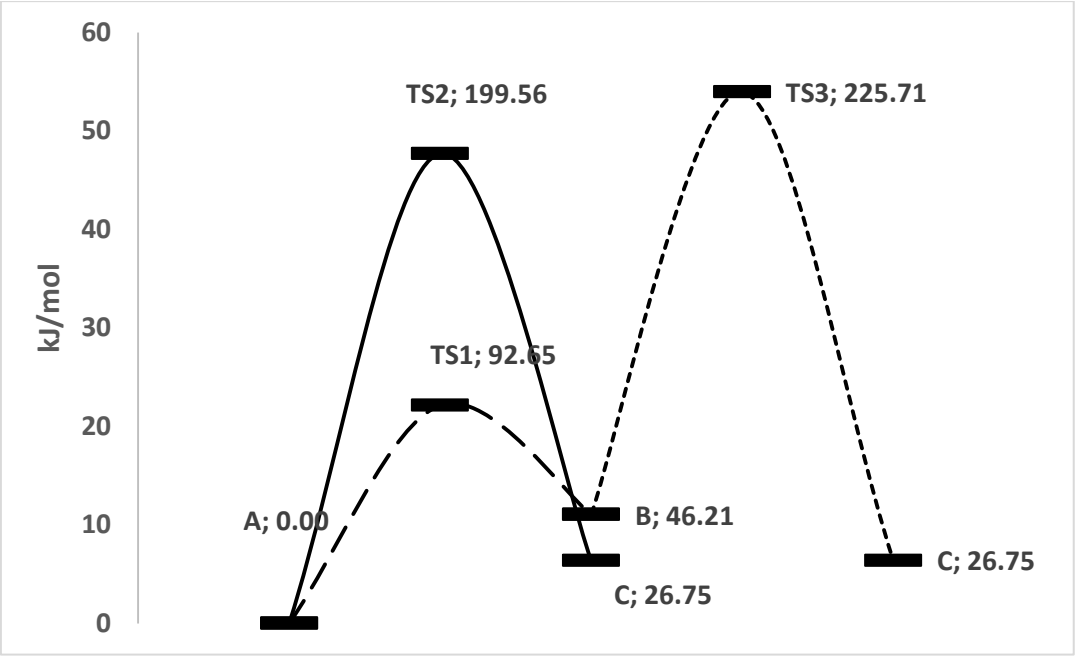

Figure 4-Overall reaction energy profiles in aqueous solution.

The thermodynamic functions based on vibrational analysis and statistical thermodynamics such as heat capacity entropy (ΔSº), enthalpy (Hº) and Gibbs free energy (Gº) were calculated and listed in Table-3. Hº, Sº and Gº are: 682.91 kJ/mol, 489.99 J/mol and 536.82 kJ/mol for tautomer (A); 683.34 kJ/mol, 493. 12 kJ/mol and 536.31 kJ/mol for tautomer B; and 682.92 kJ/mol, 492.27 J/mol and 536.15 kJ/mol for tautomer C, respectively. ΔG°_{rxn} for A ↔ B is -0.51 kJ/mol, for A ↔ C it is -0.67 kJ/mol, and for B ↔ C $\Delta G^{\circ}_{rxn}$is -0.134 kJ/mol (Table-4), this shows that tautomerization is a spontaneous process.

Conclusion

Tautomerism would highly affect chemical properties, biological properties and hence, industrial applications of azo molecules. Enol tautomer was found to be the most stable among others studied in this work. Tautomerization paths showed that A↔B and A↔C paths are thermodynamically and kinetically controlled respectively, which might be assisted by the fast hydrogen migration, this is concluded from the magnitude of the reaction rate constant. K_T and the mole fraction of the tautomers showed that enol tautomer is more abundant in tautomers mixtures of the aqueous medium, and hence, it is the more favorable.

References

1. Almeida, M.R., Stephani, R., Dos Santosh, H.F. and de Oliveira, L.F. **2010.** Spectroscopic and theoretical study of the "azo"-dye E124 in condensate phase: evidence of a dominant hydrazo form, *J. Phys. Chem. A*, **114**: 526-534.
2. Biswas, N. and Umapathy, S. **2003.** Resonance Raman study of the solvent dynamics for ultrafast charge transfer transition in 4-nitro-4′-dimethylamino-azobenzene, *J. Phys. Chem. A,* **118**: 5526-5536.
3. Ojala, W.H., Sudbeck, E.A., Lu, L.K., Richardison, T.I., Lovrien, R.E. and Gleason, W.B. **1996.** Complexes of lysine, histidine, and arginine with sulfonated azo dyes: model systems for understanding the biomolecular recognition of glycosaminoglycans by proteins, *J. Am. Chem. Soc*, **118**: 2131–2142.
4. Zinke, T. and Bindenwald, M. **1884.** Ueber phenylhydrazinderivate des α- und β-naphtochinons. identität des α-derivats mit dem azoderivat des α-naphtols. *Chem. Ber*., **17**: 3026-3033.
5. Frierz-David, H.E., Blangey, L. and Streif, H. **1946.** Zur Kenntnis der p-Oxy-azo-Farbstoffe. *Helv. Chim. Acta*, **29**: 1718.
6. Zollinger, H. **1991**. *Color chemistry: syntheses, properties and applications of organic dyes and pigments*. Weinheim: VCH.

7. Joshi, H., Kamounah, F.S., van der Zwan, G., Gooijer, C. and Antonov, L. **2001.** Temperature dependent absorption spectroscopy of some tautomeric azo dyes and Schiff bases. *J. Chem. Soc. Perkin Trans*, **2**(12):2303-2308.

8. Pavlovic, G., Racane, L., Cicak, H. and Tralic-Kulenovic, V. **2009.** The synthesis and structural study of two benzothiazolyl azo dyes: X-ray crystallographic and computational study of azo–hydrazone tautomerism. *Dyes and Pigments*, **83**: 354–362.

9. Nedeltcheva, D., Antonov, L., Lycka, A., Damyanova, B. and Popov, S. **2009.** Chemometric models for quantitative analysis of tautomeric Schiff bases and azo dyes. *Curr. Org. Chem*, **13**: 217-240.

10. Kleinpeter, E. **2000.** Recent advances in studying tautomerism in solution. *Adv. Mol. Struct Res*., **6**: 97-129.

11. Sheikhshoaie, I. and Fabian, W.M.F. **2009.** Theoretical insights into material properties of Schiff bases and related azo compounds.*Curr. Org. Chem*, **13**: 147-571.

12. Greenwood, J.R., Calkins, D., Sullivan, A.P. and Shelley, J.C. **2010.** Towards the comprehensive, rapid, and accurate prediction of the favorable tautomeric states of drug-like molecules in aqueous solution. *J. Comput. Aided Mol. Des*, **24**: 591-604.

13. Bello, I. A. and Semire, B. **2013.** Theoretical study on structural and electronic properties of 4-[(E)-[4-(trifloromethyl)-1,3-benzothiazol-2-yl]azo]naphthalen-1-ol and 1-[(E)-[4-(trifloromethyl)-1,3-benzothiazol-2-yl]azo]naphthalen-2-ol using density functional theory (DFT).*Int. J. Phys. Sci*, **8**: 1494-1505.

14. Bello, I.A., Bello, K.A., Peters, O.A. and Bello, O.S. **2009.** Synthesis, spectroscopic, thermodynamic and dyeing properties of disperse dyes derived from 2-amino-4-trifluoromethylbenzothiazole. *Report and Opinion*, **1**: 58-66.

15. Spartan user's guide, Wave function, Inc, Irvine, CA 92612 USA.

16. Becke, A.D. **1988.** Density-functional exchange-energy approximation with correct asymptotic behavior. *Phys. Rev. A*, **38**: 3098–3100.

17. Lee, C.T, Yang, W.T. and Parr, R.G. **1988.** Development of the Colle-Salvetti correlation-energy formula into a functional of the electron density. *Parr. Phys. Rev. B*, **37**: 785-589.

18. Koopmans, T. **1934.** Ordering of wave functions and eigenvalues to the individual electrons of an atom, *Physica*, **1**: 104-113

19. Parr, R.G., Szentpaly, and Liu, S. **1999.** Electrophilicity Index, *J. Am. Chem. Soc*, **121**: 1922-1924.

20. Zhou, Z. and Navangul, H.V. **1990.** Absolute hardness and aromatisity: MNDO study of benzenoid hydrocarbons. *J. Phys. Org. Chem*, **3**: 784-788.

21. Takusagawwa, F. and Shimada, A. **1976.** Isonicotinic Acid. *Acta Cryst A*., **32**: 1925-1927.

22. Chamizo, J.A., Morgado, J. and Sosa, O.**1993.** Organometallic Aromaticity.*Organometalliks*,**12**: 5005-5007.

23. Pearson, R.G. **1993.** The principle of maximum hardness. *Acc. Chem. Res*, **26**: 250-255.

24. Domingo, L.R., Aurell, M.J., Perez, P. and Conteras, R. **2002.** Quantitative characterization of the local electrophilicity of organic molecules. Understanding the regioselectivity on deals-adler reactions. *J. Phys. Chem. A*, **106**: 6871-6875.

25. De Proft, F. and Geerlings, P. **2001.** Conceptual and computational DFT in the study of aromaticity, *Chem. Rev*., **101**: 1451-1464.

26. Allen, F.H., Kennard, O., Watson, D.G., Brammer, L. and Orpen, A.G. **1987**. Tables of bond lengths determined by *X*-ray and neutron diffraction. Part 1. Bond lengths in organic compounds, *Journal of the Chemical Society Perkin Transactions II*, S1–19.

27. Sasaki, C., Kitoh, S., Yamada, K., Kunimoto, K-K., Maeda, S. and Kuwae, A., and Hanai K. **2003.** Crystal structure of 2-trifluoromethyl-40 –dimethylaminoazobenzene. *Analytical Sciences*, **19**: 1–2.

28. Teimouri, A., Chermahini, A.N. and Emami, M. **2008**. Synthesis, characterization, and DFT studies of a novel azo dye derived from racemic or optically active binaphthol. *Tetrahedron*, **64**: 11776–11782.

29. Palafox, M.A., Tardajos, G., Martines, A.G.,Rastogi, V.K., Mishra, D., Ojha, S.P. and Kiefer, W. **2007.** FT-IR, FT-Raman spectra, density functional computations of the vibrational spectra and molecular geometry of biomolecule 5-aminouracil.*Chem. Phys*., **340**: 17–31.

30. Devlin, F.J., Finley, J.W., Stephens, P.J. and Frisch, M.J. **1995**. Ab Initio Calculation of vibrational absorption and circular dichroism spectra using density functional force fields: a comparison of local, nonlocal, and hybrid density functionals. *J. Phys. Chem*., **99**: 16883-16902.
31. Erdoğan, T., Aslı, P., Davut, A. and Yusuf, A. **2009.** Theoretical studies of molecular structure and vibrational spectra of the asymmetric Squaraine [(2-dimethylamino-4-anilino) Squaraine]. *Arabian J. Sci. Engr. 2A*, **34**: 55-62.
32. Merrick, J.P., Moran, D. and Radom, L. **2007**. An evaluation of harmonic vibrational frequency scale factors. *J. Phys. Chem. A.* **111**: 11683-11700.
33. Surendra B.N. **2013.** DFT studies of molecular structure, equilibrium constant for keto-enol tautomerism and geometrical isomerism (E-Z) of 2-amino-1-phenylpropan-1-one (Cathinone).*Advances in Applied Science Research,* **4**(2): 147-153.